

Study of avalanche models using well-balanced finite volume schemes

Estudio de modelos de avalancha usando esquemas de volúmenes finitos bien balanceados

Fecha de entrega: 21 de diciembre 2022

Fecha de aceptación: 3 de abril 2023

Fernando Campos¹, Mauricio Sepúlveda¹, Rodrigo Abarca del Río² and Dieter Issler³

¹ Departamento de Ingeniería Matemática DIM and Centro de Investigación en Ingeniería Matemática CFMA, Universidad de Concepción, Concepción, Chile, fcamposg@udec.cl, maursepu@udec.cl

² Department of Geophysics, Universidad de Concepción, Concepción, Chile, rabarcadelrio@gmail.com

³ Department of Natural Hazards, Norwegian Geotechnical Institute, Oslo, Norway, Dieter.Issler@ngi.no

Avalanches are natural disasters with substantial human and economic consequences worldwide. Chile, a mountainous country, is particularly susceptible to these events. In this study, we employ a numerical technique based on the Saint-Venant system of differential equations and the well-balanced Finite Volume method with hydrostatic reconstruction to analyse snow avalanche behaviour, taking into account topography and friction as described by the Voellmy-Salm rheology model. The Rigopiano avalanche in Italy serves as a case study to test and validate our strategy, demonstrating the model's potential in simulating real-world avalanche events. The numerical model is thoroughly explained, and the results for the real avalanche case are presented visually, showing close alignment with field data and estimates from the literature. In conclusion, we highlight key findings, emphasize the importance of further research in avalanche modelling, and suggest the potential applications of these models for avalanche risk management in regions like Chile.

Keywords: avalanches, natural disasters, Saint Venant's equations, well balanced finite volumes, hydrostatic reconstruction

Las avalanchas son desastres naturales con importantes consecuencias humanas y económicas en todo el mundo. Chile, un país montañoso, es particularmente susceptible a estos eventos. En este estudio, empleamos una técnica numérica basada en el sistema de ecuaciones diferenciales de Saint-Venant y el método de volúmenes finito bien balanceado con reconstrucción hidrostática para analizar el comportamiento de las avalanchas de nieve, teniendo en cuenta la topografía y la fricción descritas por la reología del modelo de Voellmy-Salm. La avalancha de Rigopiano en Italia sirve como caso de estudio para probar y validar nuestra estrategia, demostrando el potencial del modelo para simular eventos de avalanchas del mundo real. El modelo numérico se explica detalladamente y los resultados para el caso de avalancha real se presentan visualmente, mostrando una estrecha alineación con los datos de campo y las estimaciones de la literatura. En conclusión, destacamos los hallazgos clave, enfatizamos la importancia de seguir investigando en el modelado de avalanchas y sugerimos las posibles aplicaciones de estos modelos para la gestión del riesgo de avalanchas en regiones como Chile.

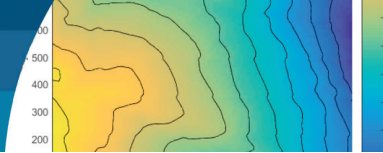
Palabras clave: avalanchas, desastres naturales, ecuaciones de Saint Venant, volúmenes finitos bien balanceados, reconstrucción hidrostática

Introduction

The effects of climate change on natural disasters are attracting considerable attention. These changes are susceptible to trigger snow avalanches. Snow avalanches are defined as the rapid descent of snow masses down steep

slopes as result of gravity, often dragging soil, rocks and vegetation (Pudasaini and Hutter, 2007).

An estimated 250 people per year fatalities are due to snow avalanches worldwide (Schweizer *et al.*, 2015). In certain regions, the economic cost to avoid the effects of snow



avalanches can be very high. For example, it is estimated that the average annual cost in Canada exceeds US\$5 billion (Schweizer *et al.*, 2015).

In Chile, there are large areas with high altitudes where snow avalanches can occur. According to published statistics on fatalities in central Chile between 1906 and 2001, of the 378 total victims, 241 (63.8%) were related to mining activities, while 52 (13.8%) were related to tourism (Ramírez and Mery, 2007).

Currently, only the mining sector in the Center-North zone uses meteorological records, data analysis, and avalanche simulation for avalanche risk management (Ramírez and Mery, 2007). In Chile, there is no governmental avalanche warning service, and only private groups such as ski resorts and mining enterprises take preventative steps.

Using a numerical model to simulate snow height and flow velocity is one method for analysing avalanche dynamics. Numerous physical models exist to describe avalanches. For this purpose, the Saint-Venant system of differential equations is widely used (Pudasaini and Hutter, 2007). The model includes friction effect as a source term. The frictional rheology model used varies depending on the fluid characteristics. Consideration will be given to the Voellmy-Salm rheology model proposed by Salm (1993) and Voellmy (1955). However, we can mention that other physical models can be used. For example, the Savage-Hutter equations of various types are used to model avalanches (Savage and Hutter, 1991). The numerical model that we use is the finite volume method, which uses a non-conservative scheme. The main approach is described by Bouchut (2004), along with the hydrostatic reconstruction scheme. This approach will be used to conduct our simulations. The scheme is well-balanced, consistent, and stable (Bouchut, 2004).

We might list a few publications that complement and work with this strategy. The hydrostatic reconstruction is utilized by Audusse (2004) for a well-balanced approach for the Saint-Venant problem with topography, including proofs and numerical examples, as well as an extension to second order. The enhanced second-order approach shown by Kurganov and Petrova (2007) preserves steady states and fluid height positivity. In reference to pyroclastic avalanches, a numerical technique using the Voellmy-Salm

rheology is discussed by de'Michieli Vitturi *et al.* (2018) along with other numerical examples.

The Rigopiano avalanche in Italy was investigated using the numerical technique in this study. There is abundant literature about this disaster, and numerous studies have been conducted in the zone to establish the event's characteristics. The meteorological conditions and fluid dynamics are detailed by Frigo *et al.* (2021). The velocity and departure distance estimates are provided by Issler (2020). We will provide graphs of the numerical simulations performed with the scheme, using estimates for the physical parameters and assumptions about the initial conditions that we consider reasonable according to the available data. Finally, we will conclude, describe various numerical approach enhancements that may be investigated, and provide some suggestions for future studies.

Methodology

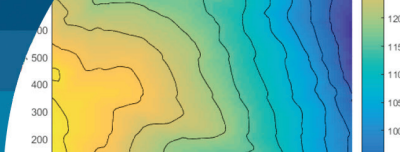
We consider the Saint-Venant system with Voellmy-Salm rheology model as avalanche model. The model is given by

$$\begin{cases} \partial_t h + \partial_x(hu) + \partial_y(hv) = 0, \\ \partial_t(hu) + \partial_x\left(hu^2 + g\frac{h^2}{2}\right) + \partial_y(huv) + gh\partial_x z = \\ \frac{u}{\sqrt{u^2 + v^2}}\left(\mu hg + \frac{g}{\xi}(u^2 + v^2)\right), \\ \partial_t(hv) + \partial_x(huv) + \partial_y\left(hv^2 + g\frac{h^2}{2}\right) + gh\partial_y z = \\ \frac{v}{\sqrt{u^2 + v^2}}\left(\mu hg + \frac{g}{\xi}(u^2 + v^2)\right), \end{cases} \quad (1)$$

where $h = h(x, y, t)$ is the fluid height, $u = u(x, y, t)$ and $v = v(x, y, t)$ are the components of the velocity, $z = z(x, y)$ is the topography height, g is the gravitational constant, μ is Coulomb's coefficient of friction (Popov, 2010) and ξ is the turbulent friction coefficient (Ferziger and Peric, 2002). We also consider the initial conditions:

$$h_0 = h(x, y, 0), \quad u_0 = u(x, y, 0), \quad v_0 = (x, y, 0) \quad (2)$$

We define $Z = gz$ and we set $U = (h, hu, hv)$ as the system solution. We have made the following assumptions for the avalanche model:



1. The avalanche can be treated as a homogeneous fluid (the density is constant in space and time).
2. The velocity in the vertical direction is negligible.
3. The pressure distribution is hydrostatic in the vertical direction.
4. The curvature of the bed is negligible.
5. Normal and shear stresses on the free surface are negligible.
6. We can consider that the bed has a gentle slope concerning the horizontal plane of reference. This means we can approximate the normal to the bed with the vertical direction.

The last assumption is not realistic in everyday avalanche events with steep terrain. However, first, we will develop the scheme for this model. Later, we will show a more accurate physical model that considers this problem. Then, we will discuss a way to adapt the numerical scheme for the new model.

In this work we use a non conservative finite volume scheme. We study this method in parts, first developing the one dimensional model, then using this scheme for the two-dimensional problem, and finally, we include friction in the model.

One-dimensional frictionless model

The one-dimensional model without friction is given by

$$\begin{cases} \partial_t h + \partial_x(hu) = 0, \\ \partial_t(hu) + \partial_x\left(hu^2 + g\frac{h^2}{2}\right) + gh\partial_x z = 0, \end{cases} \quad (3)$$

We define $U = (h, hu)$. We can write the equations as a quasi-linear system in the variable $U = (U, Z)$.

$$\begin{cases} \partial_t U + \partial_x F(U, Z) + B(U, Z)\partial_x Z = 0, \\ \partial_t Z = 0, \end{cases} \quad (4)$$

with

$$F = \begin{pmatrix} hu \\ hu^2 + g\frac{h^2}{2} \end{pmatrix}, \quad B = \begin{pmatrix} 0 \\ h \end{pmatrix}$$

We consider a critical point for this system a point (U, Z) such that $F_t(U, Z)$ is not invertible. We can write the equations in the form

$$\partial_t(U, Z) + A(U, Z)\partial_x(U, Z) = 0 \quad (6)$$

With

$$A(U, Z) = \begin{pmatrix} F_U & F_Z + B \\ 0 & 0 \end{pmatrix} \quad (7)$$

The eigenvalues of $A(U, Z)$ are:

$$\lambda_1 = u - \sqrt{gh}, \quad \lambda_2 = 0, \quad \lambda_3 = u + \sqrt{gh} \quad (8)$$

Then, we have that at every noncritical point, the system is hyperbolic ($A(U, Z)$ is diagonalizable). The stationary states are the solutions $U(x)$ independent of time. These states are relevant because generally represent the solution when time tend to infinity. The stationary states are the functions $h(x)$ and $u(x)$ that satisfy:

$$\begin{cases} hu = \text{cte.}, \\ \frac{u^2}{2} + gh + Z = \text{cte.}, \end{cases} \quad (9)$$

The stationary states at rest are given by

$$\begin{cases} u = 0, \\ h + z = \text{cte.} \end{cases} \quad (10)$$

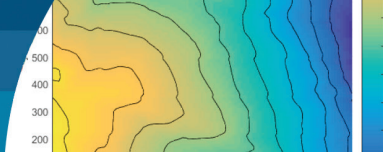
In the finite volume method, a mesh of points $x_{i+1/2}$, $i \in \mathbb{Z}$, in space is created. Finite volumes are defined by $C_i =]x_{i-1/2}, x_{i+1/2}[$. We consider a time step Δt and define $t_{n+1} = t_n + \Delta t$, $n \in \mathbb{N}$. We want to approximate the solution $U(x, t)$ by discrete values U_i^n , $i \in \mathbb{Z}$, $n \in \mathbb{N}$. This is,

$$U_i^n \approx \frac{1}{\Delta x_i} \int_{C_i} U(t_n, x) dx \quad (11)$$

We consider a first order non conservative finite volume scheme given by

$$U_i^{n+1} - U_i^n + \frac{\Delta t}{\Delta x_i} (F_{i+1/2-} - F_{i-1/2}) = 0 \quad (12)$$

with



$$F_{i+1/2-} = F_l(\tilde{U}_i^n, \tilde{U}_{i+1}^n), \quad F_{i+1/2+} = F_r(\tilde{U}_i^n, \tilde{U}_{i+1}^n) \quad (13)$$

where $\tilde{U}_i^n = (U_i^n, Z_i)$, and F_l and F_r are the left and right numerical fluxes, respectively.

We impose a Courant-Friedrichs-Lewy (CFL) condition for the time step to allow the convergence of the numerical model. The condition has the following form

$$\Delta t a \leq \Delta x \quad (14)$$

where $a = \max|\lambda|$, is the maximum modulus of the eigenvalues of the matrix system, evaluated for all cells at time step n (Audusse, 2004).

A well balanced scheme for this problem is the hydrostatic reconstruction scheme (Bouchut, 2004). Considering the topography, to calculate the fluxes between the mesh elements it is necessary to reconstruct the left and right solution states at each interface. We denote this states $U_l = (h_l, hu_l)$ and $U_r = (h_r, hu_r)$, and reconstructed states as $U_l^* = (h_l^*, hu_l^*)$ and $U_r^* = (h_r^*, hu_r^*)$, respectively.

In the hydrostatic reconstruction scheme, the steady state relations are replaced by

$$\begin{cases} u = \text{cte.}, \\ gh + Z = \text{cte.}, \end{cases} \quad (15)$$

With these relations, the reconstructed states are obtained by

$$\begin{aligned} gh_l^* &= (gh_l - (\Delta Z)_+)_+, \\ gh_r^* &= (gh_r - (-\Delta Z)_+)_+, \end{aligned} \quad (16)$$

where $\Delta Z = Z_r - Z_l$. The fluxes will be given by

$$\begin{aligned} F_l(U_l, U_r, Z_l, Z_r) &= \mathcal{F}(U_l^*, U_r^*) \\ &+ \begin{pmatrix} 0 \\ \frac{gh_l^2}{2} - \frac{g(h_l^*)^2}{2} \end{pmatrix} \\ F_r(U_l, U_r, Z_l, Z_r) &= \mathcal{F}(U_l^*, U_r^*) \\ &+ \begin{pmatrix} 0 \\ \frac{gh_r^2}{2} - \frac{g(h_r^*)^2}{2} \end{pmatrix} \end{aligned} \quad (17)$$

where \mathcal{F} is a consistent numerical flux for the Saint-Venant problem without topography. In our case, we will use the Lax-Friedrichs flux, given by

$$\mathcal{F}(U_l, U_r) = \frac{1}{2}(F(U_l) + F(U_r)) - \frac{\Delta x_i}{2\Delta t}(U_r - U_l) \quad (18)$$

It can be proven that with this flux, the scheme is conservative in h , preserves the non-negativity of h in the interface, and is well balanced, consistent and stable. Further details and technical explanations of concepts and the proofs of these propositions are presented by Bouchut (2004).

Two-dimensional frictionless model

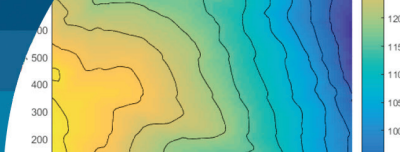
Now we can proceed with the avalanche model in two dimensions without friction force. The two-dimensional Saint-Venant problem with frictionless topography is given by

$$\begin{cases} \partial_t h + \partial_x(hu) + \partial_y(hv) = 0, \\ \partial_t(hu) + \partial_x\left(hu^2 + g\frac{h^2}{2}\right) \\ + \partial_y(huv) + gh\partial_x z = 0, \\ \partial_t(hv) + \partial_x(huv) + \\ \partial_y\left(hv^2 + g\frac{h^2}{2}\right) + gh\partial_y z = 0, \end{cases} \quad (19)$$

The solutions of the system can develop discontinuities, which means we have to consider weak solutions. These solutions are well defined under the assumption that the topography $z \in W^{1,\infty}(\mathbb{R})$ (Dafermos, 2000). To find a unique physical solution we use an entropy condition as an additional admissibility criteria. The details of the theory about uniqueness of solution are explained by Fjordholm *et al.* (2011). For the finite volume method, we consider a mesh of elements C_i in two dimensions. Let Γ_{ij} be the edge between the volumes C_i and C_j , and n_{ij} the unitary normal vector with orientation from C_i to C_j . Let U_i^n be the values of the solution in some interior point of the element C_i at time t_n . The finite volume method is given by

$$U_i^{n+1} - U_i + \frac{\Delta t}{|C_i|} \sum_{j \in K_i} |\Gamma_{ij}| F_{ij} = 0 \quad (20)$$

where $|C_i|$ is the area of the control volume C_i , $|\Gamma_{ij}|$ is the length of the edge Γ_{ij} , K_i is the set of indices of the cells that share edges with C_i , and F_{ij} is the flux between C_i and C_j with



$$F_{ij} = F(U_i, U_j, Z_i, Z_j, n_{ij}) \quad (21)$$

Let $n = (n_1, n_2)$ be the unit vector with its rotation matrix given by

$$R_n = \begin{pmatrix} n_1 & -n_2 \\ n_2 & n_1 \end{pmatrix} \quad (22)$$

Let $x' = R_n x$ and $(u', v') = R_n^{-1}(u, v)$. Then $U' = (h, hu', hv')$ is a solution to the two-dimensional problem. We can compute the numerical fluxes through the following one-dimensional problem

$$\begin{cases} \partial_t h + \partial_x(hu) = 0 \\ \partial_t(hu) + \partial_x\left(hu^2 + g\frac{h^2}{2}\right) + gh\partial_x z = 0 \\ \partial_t(hv) + \partial_x(huv) = 0 \end{cases} \quad (23)$$

Let $F_l(U'_l, U'_r, \Delta Z) = (F_l^0, F_l^1, F_l^2)$ be the flux obtained from the one-dimensional problem with U' . Then the left flux of the original two dimensional problem is given by

$$F_l(U_l, U_r, \Delta Z, n) = \begin{pmatrix} F_l^0(U'_l, U'_r, \Delta Z) \\ R_n \begin{pmatrix} F_l^1(U'_l, U'_r, \Delta Z) \\ F_l^2(U'_l, U'_r, \Delta Z) \end{pmatrix} \end{pmatrix} \quad (24)$$

Let $(h, hu, hv)^* = (h, -hu, -hv)$. By symmetry we have

$$F_r(U_l, U_r, \Delta Z) = -F_l(U_r^*, U_l^*, -\Delta Z)^* \quad (25)$$

The right flux of the original two dimensional problem is given by

$$-F_r(U_r, U_l, -\Delta Z, n) = \begin{pmatrix} F_r^0(U'_l, U'_r, \Delta Z) \\ R_n \begin{pmatrix} F_r^1(U'_l, U'_r, \Delta Z) \\ F_r^2(U'_l, U'_r, \Delta Z) \end{pmatrix} \end{pmatrix} \quad (26)$$

Now we explain how we solve the one-dimensional problem in (23).

We can obtain the numerical flux for the problem with the first and second equation with the method for one-dimensional problems shown in the previous section. The third equation is a passive transport equation

$$\partial_t(hv) + \partial_x(huv) = 0 \quad (27)$$

We obtain the flux for this part using

$$F_l^2 = \begin{cases} F_l^0 v_l & \text{if } F_l^0 \geq 0, \\ F_l^0 v_r & \text{if } F_l^0 \leq 0, \end{cases} \quad (28)$$

And analogously with F_r^2 .

Two-dimensional model with friction

Now we can consider the two-dimensional problem with friction given by (1). Friction in the Voellmy-Salm rheological model includes two parts:

1. Coulomb friction:

$$F_c = \frac{(u, v)}{\sqrt{u^2 + v^2}} (\mu h g) \quad (29)$$

2. Turbulent friction:

$$F_t = \frac{(u, v)}{\sqrt{u^2 + v^2}} \left(\frac{g}{\xi} (u^2 + v^2) \right) \quad (30)$$

Each type of friction is treated differently in the numerical scheme. We can include the Coulomb friction in the numerical method by modifying the source term in our scheme. To do this, the numerical fluxes are computed with

$$F_{ij} = F(U_i, U_j, \Delta Z_{ij} - f_1^{ij}(x_j - x_i)_1 - f_2^{ij}(x_j - x_i)_2, n_{ij}) \quad (31)$$

where x_i and x_j are arbitrary points in the interior of the elements C_i and C_j , respectively. We define

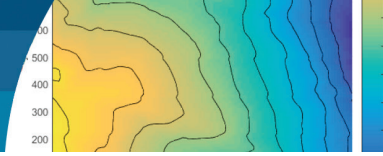
$$f^{ij} = -\varphi_{g\mu} \left((gh_i - gh_j - \Delta Z_{ij}) \frac{x_j - x_i}{|x_j - x_i|^2}, \frac{(u^{ij}, v^{ij})}{\Delta t} \right) \quad (32)$$

In the above expression, we use

$$u^{ij} = \frac{h_i u_i + h_j u_j}{h_i + h_j}, \quad v^{ij} = \frac{h_i v_i + h_j v_j}{h_i + h_j} \quad (33)$$

$$\varphi_{g\mu}(X, Y) = \text{proj}_{g\mu} \left(\text{proj}_{g\mu}(X) + \frac{2}{1 + \max(1, -X \cdot Y / g\mu|Y|)} Y \right) \quad (34)$$

For the turbulent friction, we use a splitting method to ensure the scheme stability (Bouchut *et al.*, 2020). Once the solution of the finite volume method is obtained, which we will denote as h^*, u^*, v^* , we proceed to include the turbulent friction. The final solution is given by



$$\begin{aligned} h &= h^* \\ u &= \frac{u^* h^* \xi}{g \sqrt{w^* \Delta t} + h^* \xi} \\ v &= \frac{v^* h^* \xi}{g \sqrt{w^* \Delta t} + h^* \xi} \end{aligned} \quad (36)$$

where $w = u^2 + v^2$.

Model in global coordinates

As we explained before, the model studied considers a smooth slope. In real situations, this assumption can be unsatisfactory. A way to solve this problem is to use a model in global coordinates that considers the effect on vertical velocity given by steep terrain. The scheme derived from this flow analysis is explained in detail by Zugliani and Rosatti (2021). In Figure 1 we show a control volume for the one-dimensional model with a slope angle θ .

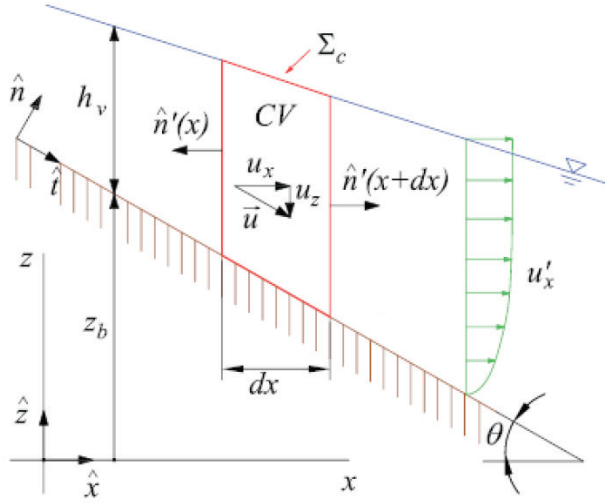


Figure 1: Control volume (x is horizontal axis and z is vertical axis). h_v is the height of the fluid, z_b is the height of the terrain topography and u_x is the velocity component in x

The system of equations in global coordinates is given by

$$\begin{cases} \partial_t h_v + \partial_x (h_v u_x) = 0, \\ \partial_t (h_v u_x) + \partial_x \left(h_v u_x^2 + g \cos^2 \theta \frac{h_v^2}{2} \right) \\ + g \cos^2 \theta h_v \partial_x z_b = -\frac{\tau_0}{\rho} \frac{s_x^\tau}{\cos \theta} \end{cases} \quad (37)$$

where

$$\frac{\tau_0}{\rho} = \mu g h_v \cos^2 \theta + g \frac{u_x^2}{\xi \cos^2 \theta} \quad (38)$$

$$s_x^\tau = \frac{u_x}{|u_x|} \cos \theta \quad (39)$$

This model can be extended to two dimensions, giving the following system

$$\begin{cases} \partial_t h_v + \partial_x (h_v u_x) + \partial_y (h_v u_y) = 0 \\ \partial_t (h_v u_x) + \partial_x \left(h_v u_x^2 + g \cos^2 \theta \frac{h_v^2}{2} \right) + \partial_y (h_v u_x u_y) \\ + g \cos^2 \theta h_v \partial_x z_b = \frac{u_x}{|u|} \left(\mu g h_v \cos^2 \theta + g \left(\frac{u_x^2 + u_y^2}{\xi \cos^2(\theta)} \right) \right) \\ \partial_t (h_v u_y) + \partial_x (h_v u_x u_y) + \partial_y \left(h_v u_y^2 + g \cos^2 \theta \frac{h_v^2}{2} \right) \\ + g \cos^2 \theta h_v \partial_x z_b = \frac{u_y}{|u|} \left(\mu g h_v \cos^2 \theta + g \left(\frac{u_x^2 + u_y^2}{\xi \cos^2(\theta)} \right) \right) \end{cases} \quad (40)$$

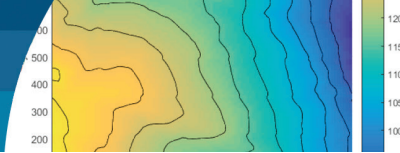
We can rewrite this system in the form of the avalanche model (1) as follows

$$\begin{cases} \partial_t h_v + \partial_x (h_v u_x) + \partial_y (h_v u_y) = 0 \\ \partial_t (h_v u_x) + \partial_x \left(h_v u_x^2 + \tilde{g} \frac{h_v^2}{2} \right) + \partial_y (h_v u_x u_y) \\ + \tilde{g} h_v \partial_x z_b = \frac{u_x}{|u|} \left(\mu \tilde{g} h_v + \frac{\tilde{g}}{\xi} (u_x^2 + u_y^2) \right) \\ \partial_t (h_v u_y) + \partial_x (h_v u_x u_y) + \partial_y \left(h_v u_y^2 + \tilde{g} \frac{h_v^2}{2} \right) \\ + \tilde{g} h_v \partial_x z_b = \frac{u_y}{|u|} \left(\mu \tilde{g} h_v + \frac{\tilde{g}}{\xi} (u_x^2 + u_y^2) \right) \end{cases} \quad (41)$$

where $\tilde{g} = g \cos^2 \theta$ and $\xi = \cos^2 \theta$. In this way we can use the hydrostatic reconstruction method for this system with the new parameters \tilde{g} and ξ . We recall that this method allows incorporating the Coulomb friction. In the case of turbulent friction, it is added by means of splitting, and to do so the original parameter g is used, as can be seen from the system of equations.

Results

The numerical scheme was applied for the case of the snow avalanche of January 18, 2017 at Rigopiano, Gran Sasso National Park (Frigo *et al.*, 2020). This natural disaster



destroyed the Rigopiano hotel, resulting in the death of 29 people. The avalanche was a mixture of snow and wood, displacing rocks and trees in its path. The damage generated in the event shows that the avalanche was of great intensity. Figure 2 shows an aerial view of the path of the avalanche before and after the event.

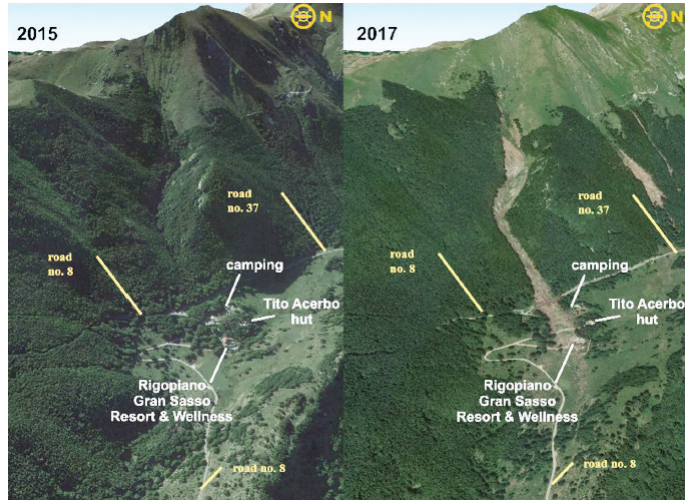


Figure 2: Aerial view of the path of the avalanche over Rigopiano Hotel, before (2015) and after (2017) the catastrophic event. The image is taken from Frigo *et al.* (2020)

Figure 3 shows a map of the Abruzzo region, where the avalanche happened. The position of the Rigopiano Hotel is indicated. The location of snow measurement points in the area is also shown. We also show a map of Italy with the position of the Abruzzo region.

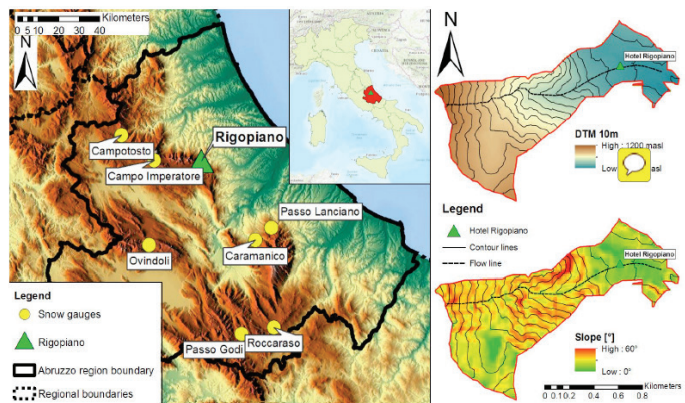


Figure 3: Geographical area of the Abruzzo region with the Rigopiano Hotel (green triangle) position. Snow gauges in the area are also shown (yellow circles). Italy map on top with Abruzzo region marked in red. The right diagrams show the relief's height and slope, indicating the avalanche's main flow. The image is taken from Bocchiola *et al.* (2020).

A simulation of the avalanche at Rigopiano using the system of equations in global coordinates given in (41) is now presented. The numerical method consists of finite volumes with a hydrostatic reconstruction scheme, with the parameters for the new physical model being modified. Figure 4 displays the topography z of the Rigopiano area under study.

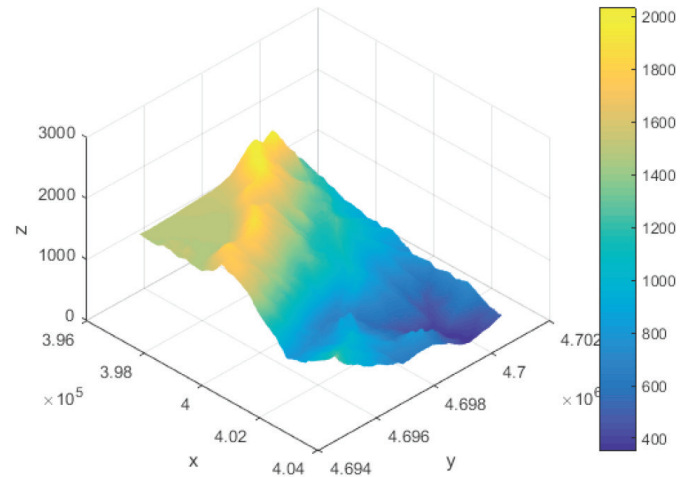


Figure 4: Rigopiano topography with height z . This surface is considered as the relief without snow of the area. Right scale is given in m

We worked with a sub-domain of this domain for the numerical simulation, based on the area shown in the Figure 3. This sub-domain's dimensions are approximately 989 m x 989 m, with approximate coordinates in Figure 4 given by $[4.0001 \cdot 10^5, 4.0100 \cdot 10^5], [4.6970 \cdot 10^6, 4.6980 \cdot 10^6]$. The topography in this sub-domain is shown in Figure 5.

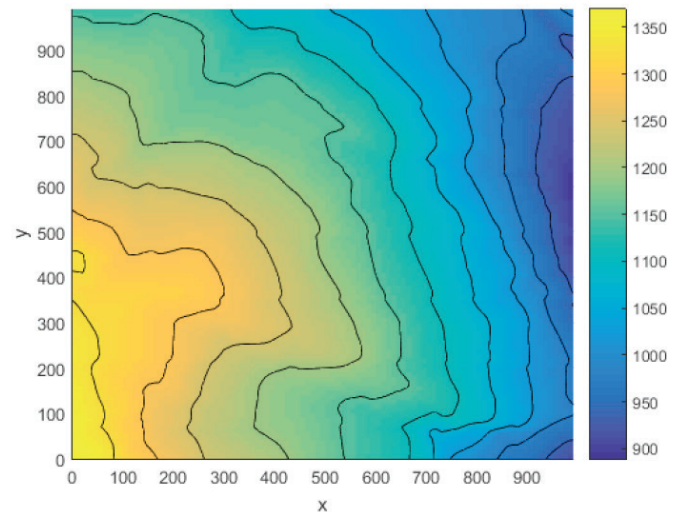
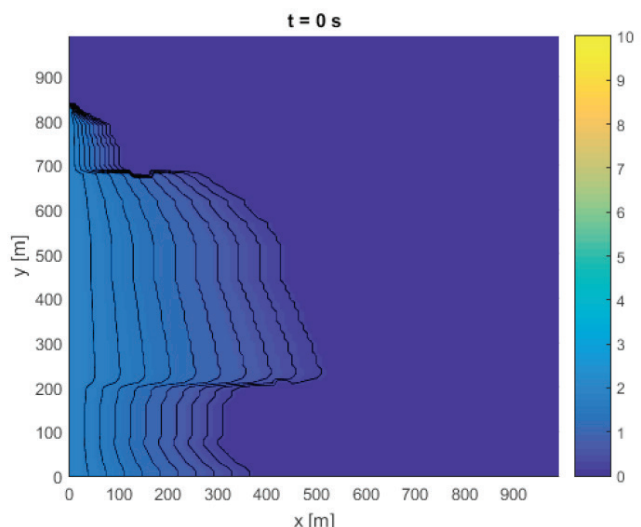
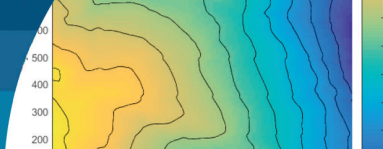
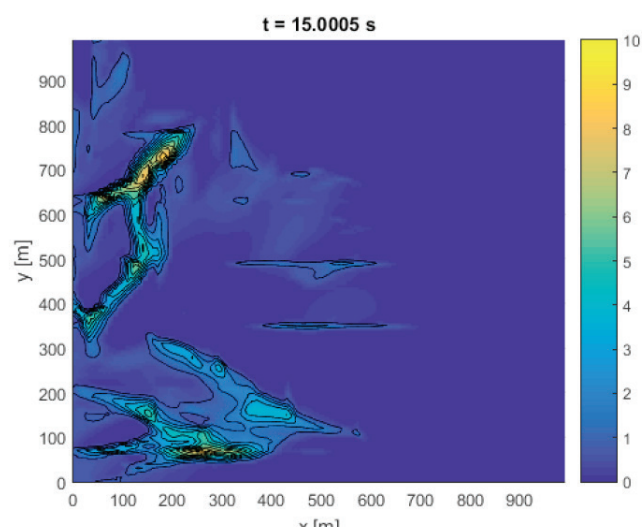


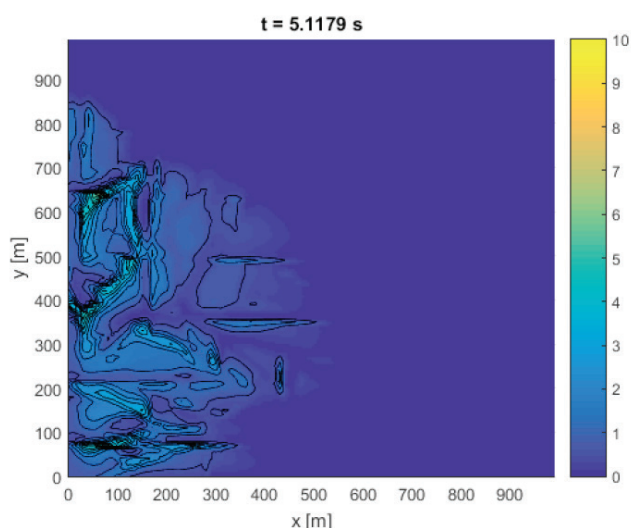
Figure 5: Topography in sub-domain with height z . The isolevels are shown. Right scale is given in m



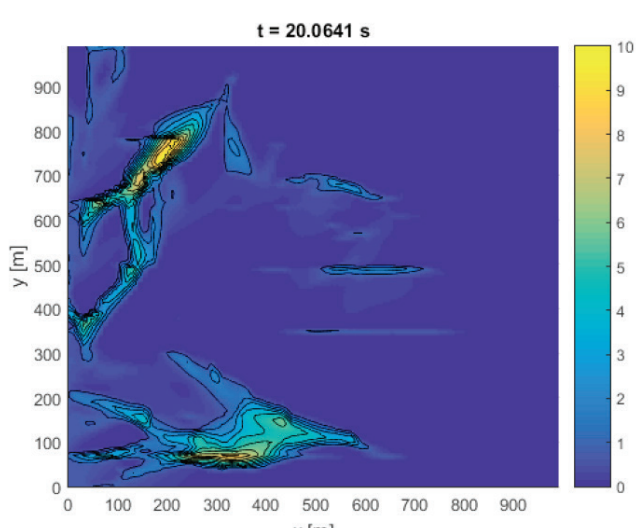
a) Simulation at $t = 0$ s.



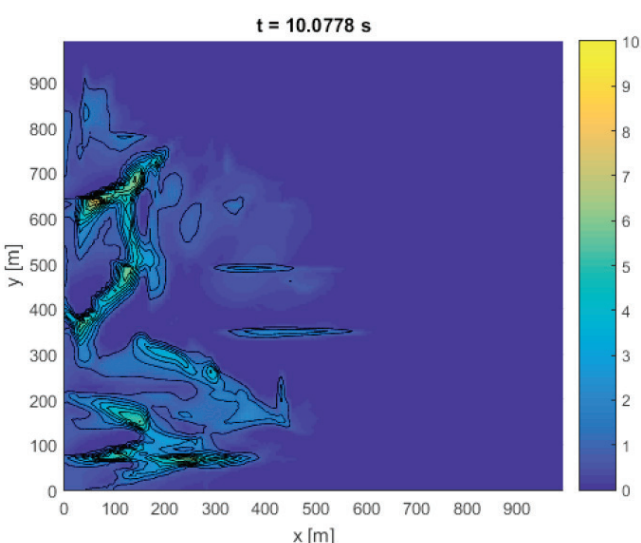
d) Simulation at $t = 15$ s.



b) Simulation at $t = 5$ s.



e) Simulation at $t = 20$ s.



c) Simulation at $t = 10$ s.

Figure 6: Numerical simulation of the avalanche at Rigopiano at different times. The snow depth h is shown with the isovels. The scale is in m.

The initial condition for the snow height is considered to be a constant slope with a maximum height of 2 m that goes to 0 m at the isovalue $z = 1600$ m. As data we used $g = 9.8$ m/s², $\mu = 0.15$, $k = g/\xi = 0.002$ and an angle of slope $\theta = 30$. Figures 6 show the results at different times.

The model we use is the Saint-Venant system with Voellmy-Salm rheology model in global coordinates. The numerical scheme we use is the finite volume method with hydrostatic reconstruction scheme.

The domain used for this simulation is the closer to the real avalanche for the initial snow depth and for the flux behaviour.

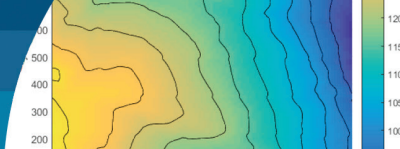


Figure 6a) shows the initial condition. Because the lack of data, we made a reasonable assumption for this condition, with a constant slope with a maximum height of 2 m.

We can see the snow advance in the direction of the slope of the topography, which is the expected result for the avalanche simulation.

Conclusions

In this comprehensive study, we have modelled an avalanche by employing the Saint-Venant system of differential equations, considering topography and friction as described by the Voellmy-Salm rheology model. The finite volume method, with hydrostatic reconstruction, has been utilized to examine a real-world scenario. Our methodology was rigorously tested using various examples from the literature, spanning one-dimensional and two-dimensional cases, as well as both frictional and frictionless scenarios. This comprehensive testing enabled us to calibrate and validate the numerical model, ensuring its accuracy and reliability.

The primary focus of our investigation centred on the Rigopiano avalanche, a real-life event that highlights the importance of steep terrain in determining avalanche outcomes. To accurately model this event, it was crucial to account for the impact of such conditions on flow dynamics and incorporate these effects into the system of equations. While specific information regarding initial snow depth was unavailable, we reasonably assumed a maximum snow height of 2 m. Furthermore, we were able to make well-founded estimations of friction characteristics and slope angle (30 degrees) for the system based on relevant literature and research.

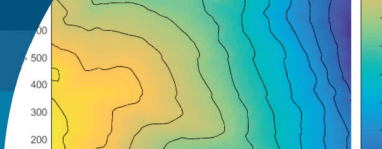
Initially, we chose a smaller domain for our simulations but later discovered that the actual avalanche had originated near the edge of the original domain. By adjusting our model accordingly, we significantly improved the accuracy of our initial numerical results. Our refined model now demonstrates that the snow flux closely aligns with the field data collected at Rigopiano, and the snow velocity is consistent with estimates found in the literature. While more precise data would allow for an even more accurate comparison with the actual avalanche, our initial numerical model offers a reasonable simulation of snow behaviour as a first approach.

Moving forward, there are several possible improvements to be considered. For instance, we could explore more sophisticated physical models that improve the flow characteristics of avalanches. Moreover, it is worth investigating the use of more precise numerical models, particularly regarding the incorporation of friction and the impact of slope angle on velocity. We employed a Lax-Friedrichs flux for the numerical scheme and hydrostatic reconstruction, which is straightforward to implement but suffers from excessive numerical dissipation. This limitation can be mitigated by substituting the flux with an upwind HLLC flux and applying second-order extensions using the Osher-Solomon-Toro Riemann solver. We are currently conducting numerical experiments in this area, which could potentially lead to future research.

In Chile, there is significant potential for the application of avalanche-related research, particularly as rising temperatures increasingly impact the region. To address these hazards, it is crucial to employ a variety of investigative methods. Numerical models, such as the one presented in this study, can complement field observations and laboratory research, contributing to a more comprehensive understanding of avalanche dynamics. There are many opportunities for further research in this field in Chile, since developing and refining these models can lead to more effective avalanche prediction and mitigation strategies.

To our knowledge, this study represents the first of its kind in Chile, and we anticipate that the ideas presented here will be further enhanced and applied to other real-world situations in the near future. As research in this area progresses, it has the potential to significantly improve avalanche risk management, ultimately contributing to the safety and well-being of communities in avalanche-prone regions. By enhancing our understanding of avalanche behaviour and refining the predictive capabilities of our numerical models, we can develop more effective and targeted strategies for avalanche prevention, preparedness, and response.

In conclusion, this work demonstrates the potential of using the Saint-Venant system of differential equations, coupled with the finite volume method and hydrostatic reconstruction, to model avalanches accurately. Our initial model has shown promising results in simulating the Rigopiano avalanche, and with further improvements, it can provide



valuable insights into the behaviour of avalanches in various environments. As we refine these models and explore their applications, we can better understand the complex dynamics of avalanches, ultimately working towards more effective avalanche risk management strategies and protecting communities in avalanche-prone areas.

Acknowledgements

F. Campos gratefully acknowledge the funding from FONDECYT 1180868. Research of M. Sepúlveda was supported FONDECYT Grant No. 1220869, ANID project ECOS200018, and by Centro de Modelamiento Matemático (CMM), ACE210010 and FB210005, BASAL funds for centers of excellence from ANID-Chile. Special thanks to Dr. Francois Bouchut for his helpful comments on the computational implementation of the Voellmy-Salm friction term.

References

- Audusse, E., Bouchut, F., Bristeau, M.O., Klein, R. and Perthame, B.T. (2004). A fast and stable well-balanced scheme with hydrostatic reconstruction for shallow water flows. *SIAM Journal on Scientific Computing* 25(6), 2050-2065
- Bocchiola, D., Galizzi, M., Bombelli, G.M. and Soncini, A. (2018). Mapping snow avalanches hazard in poorly monitored areas. The case of Rigopiano avalanche, Apennines of Italy. *Natural Hazards and Earth System Sciences* (discussion), 1-31
- Bouchut, F. (2004). *Nonlinear stability of finite volume methods for hyperbolic conservation laws and well-balanced schemes for sources*. Birkhäuser Verlag, Basel, Switzerland
- Bouchut, F., Fernández-Nieto, E.D., Koné, E.H., Mangeney, A. and Narbona-Reina, G. (2021). Dilatancy in dry granular flows with a compressible $\mu(I)$ rheology. *Journal of Computational Physics* 429, 110013
- Dafermos, C.M. (2000). *Hyperbolic conservation laws in continuum physics*. Springer, Berlin, Germany
- de' Michieli Vitturi, M., Esposti Ongaro, T., Lari, G. and Aravena, A. (2019). IMEX_SfloW2D 1.0: a depth-averaged numerical flow model for pyroclastic avalanches. *Geoscientific Model Development* 12(1), 581-595
- Ferziger, J.H., Peric, M. and Street, R.L. (2002). *Computational methods for fluid dynamics*. Springer Cham, Switzerland
- Fjordholm, U.S., Mishra, S. and Tadmor, E. (2011). Well-balanced and energy stable schemes for the shallow water equations with discontinuous topography. *Journal of Computational Physics* 230(14), 5587-5609
- Frigo, B., Bartelt, P., Chiaia, B., Chiambretti, I. and Maggioni, M. (2021). A reverse dynamical investigation of the catastrophic wood-snow avalanche of 18 January 2017 at Rigopiano, Gran Sasso National Park, Italy. *International Journal of Disaster Risk Science* 12, 40-55
- Issler, D. (2020). The 2017 Rigopiano avalanche—dynamics inferred from field observations. *Geosciences* 10(11): 466, 1-34
- Kurganov, A. and Petrova, G. (2007). A second-order well-balanced positivity preserving central-upwind scheme for the Saint-Venant system. *Communications in Mathematical Sciences* 5(1), 133-160
- Popov, V.L. (2010). *Contact mechanics and friction*. Springer Berlin Heidelberg, Germany
- Pudasaini, S.P. and Hutter, K. (2007). *Avalanche dynamics: dynamics of rapid flows of dense granular avalanches*. Springer Berlin, Heidelberg, Germany
- Ramírez, L. and Mery, J. (2007). Las avalanchas en Chile: efectos y sistemas de control. *Revista de la Construcción* 6(1), 48-63
- Salm, B. (1993). Flow, flow transition and runout distances of flowing avalanches. *Annals of Glaciology* 18, 221-226
- Savage, S.B. and Hutter, K. (1991). The dynamics of avalanches of granular materials from initiation to runout. Part I: Analysis. *Acta Mechanica* 86, 201-223
- Schweizer, J., Bartelt, P. and van Herwijnen, A. (2015). Snow avalanches. In *Snow and Ice-Related Hazards, Risks, and Disasters*, J.F. Shroder, W. Haeberli and C. Whiteman (eds.), Academic Press, Elsevier, 346–395
- Voellmy, A. (1955). Über die Zerstörungskraft von Lawinen (on the destructive force of avalanches). *Schweizerische Bauzeitung* 73, 212-217
- Zugliani, D. and Rosatti, G. (2021). TRENT2D: An accurate numerical approach to the simulation of two-dimensional dense snow avalanches in global coordinate systems. *Cold Regions Science and Technology* 190, 103343